

# THE INTERACTION OF THE MONTHLY MEAN FLOW AND LARGE-SCALE TRANSIENT EDDIES IN TWO DIFFERENT CIRCULATION TYPES

Part II: Vorticity and temperature balance

by

HANNU SAVIJÄRVI

Department of Meteorology  
University of Helsinki\*)

## Abstract

The monthly mean vorticity and temperature balance was studied in high and low (blocking) index cases based on NMC numerical analyses above the 850 mb level. In the mean vorticity balance the effect of large-scale Reynolds stresses was found important, mainly cyclonic in middle latitudes but locally very variable and basically similar in both cases. For the mean temperature balance the effect of the eddies (divergence of the transient heat flux) differed more between the two cases. The horizontal distributions of the two forcing fields bore, however, some resemblance. The mixing coefficient  $K$  for the transient heat flux was positive and related to the kinetic energy of the transients while the rotational coefficient  $R$  (Clapp, [4]) was mainly negative.

## 1. Introduction

An important part of the dynamics of time-mean atmospheric flow lies in a two-way interaction with shorter period transients. This interaction in the equations of motion and the kinetic energy balance was examined diagnostically in different circulation types in Part I (SAVIJÄRVI, [16]) for two one-month periods.

In the present study the same data are used for studying the observed balance conditions of the time-mean vorticity and temperature fields. The importance of

---

\*)Present address: ECMWF, Bracknell, UK

the transients in the balance and the sensitivity to the mean circulation pattern is investigated. The transients – anomalies from the time-mean state – may arise for different physical reasons, but the main contributions over a one-month period come from moving disturbances.

The time-mean vorticity balance has been studied relatively little (*c.f.* SALTZMANN, [15], HOLOPAINEN, [7]) in spite of the fact that quasigeostrophy is one of the dominant features in large-scale atmospheric flow, and that the quasigeostrophic vorticity equation has been extensively used for both studies and short-range numerical weather prediction. The temperature balance, on the other hand, has been studied a great deal for longer time scales, especially the mean diabatic heating, which is the driving force of the general circulation (*c.f.* PEIXOTO, [11], CLAPP, [3], NEWELL, *et al.*, [9]).

The parametrization of the transient phenomena is crucial for good statistical-dynamical models of general circulation and climate. This is discussed on the basis of results obtained in two case studies.

## 2. Data

Numerical height and temperature analysis data from the National Meteorological Center (NMC) were used and all calculations were made in the NMC octagonal grid in the polar stereographic map projection using centred differences, geostrophic wind approximation and simple arithmetic time mean values for two one-month periods.

The two periods were chosen from the same year (1965), the »high zonal index» case (12/65) covering December (62 analyses) and the »low index» or blocking case (2/65) roughly covering February (28.1–28.2; 63 analyses). The high index case data includes nine pressure levels from 850 mb to 100 mb while the blocking case contains five levels, 850–200 mb. Fig. 1 shows the monthly mean height fields  $\bar{z}$  averaged with respect to available pressure levels. The blocking anticyclone was a steady and dominant feature of all pressure levels in the blocking case throughout the period. In the mean temperature field (Fig. 7) it is seen as a large warm ridge over the eastern Atlantic.

## 3. Vorticity balance and vertical velocity

The vorticity equation for the time-mean flow is similar to the normal version, with instantaneous values replaced by their time-mean values, plus an extra term  $\hat{k} \cdot \nabla \times A_H$ , which is the vorticity forcing due to transient effects:

$$\frac{\partial \bar{\eta}}{\partial t} = -\bar{V} \cdot \nabla \bar{\eta} + \hat{k} \cdot \nabla \times A_H + \bar{\eta} \frac{\partial \bar{\omega}}{\partial p} + \left( \overline{\eta' \frac{\partial \omega'}{\partial p}} - \bar{\omega} \frac{\partial \bar{\eta}}{\partial p} + \hat{k} \cdot \overline{\frac{\partial V}{\partial p} \times \nabla \omega} + \hat{k} \cdot \nabla \times \bar{F} \right) \quad (3.1)$$

$$A_H = A_x \hat{i} + A_y \hat{j} \quad \begin{cases} A_x = -\nabla \cdot \overline{u'V'} \\ A_y = -\nabla \cdot \overline{v'V'} \end{cases}$$

$\hat{k} \cdot \nabla \times A_H$  is approximately the convergence of horizontal vorticity flux associated with transient motion. The components of the horizontal interaction vector  $A_H$  in (3.1) (Part I, Eq. 3.3) also include covariances due to metric terms depending on the horizontal coordinate system chosen. The terms in brackets in Eq. 3.1 are generally small at middle and high latitudes above the boundary layer. The time change of long time-mean vorticity is also small and thus the time-mean vorticity balance can be written as a quasitriplic balance:

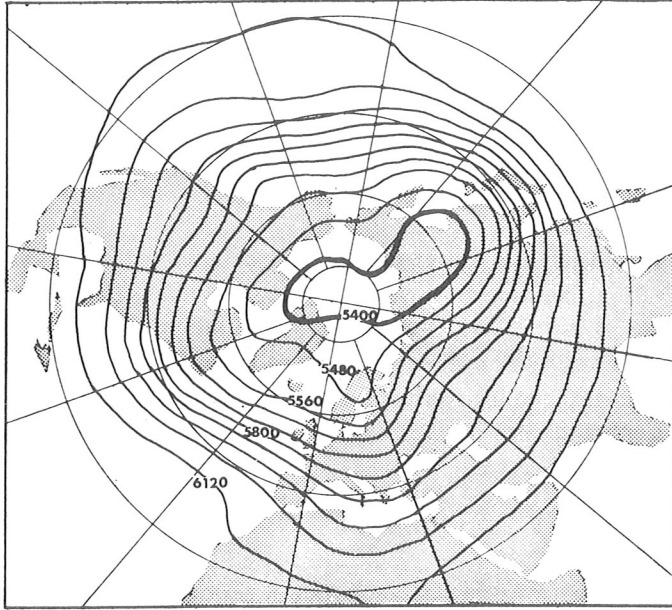
$$-\bar{V} \cdot \nabla \bar{\eta} + \hat{k} \cdot \nabla \times A_H + \bar{\eta} \frac{\partial \bar{\omega}}{\partial p} = 0 \quad (3.2)$$

When the mean advection  $-\bar{V} \cdot \nabla \bar{\eta}$  and the forcing  $\hat{k} \cdot \nabla \times A_H$  do not balance each other, there must be a compensating time-mean vertical velocity field  $\bar{\omega}$  approximately fulfilling Eq. 3.2. The vertical velocity has to vanish in the upper and lower boundaries, and if the mean advection and forcing are known *e.g.* by observations, Eq. 3.2 determines  $\bar{\omega}$  (»the vorticity method»). This boundary value problem is solved here by fitting vertically in every grid point a fourth degree polynomial  $\bar{\omega}(p)$  with the boundary values  $\bar{\omega} = 0$  at  $p = 1000$  mb and at  $p = 0$  mb. This technique is similar to that used by PERRY [14]. It is possible to use the obtained  $\bar{\omega}$ -values in the small terms of Eq. 3.1 and calculate a better approximation of  $\bar{\omega}$ . This iterative process yielded results generally only slightly different from the »quasi-geostrophic»  $\bar{\omega}$  at middle and high latitudes.

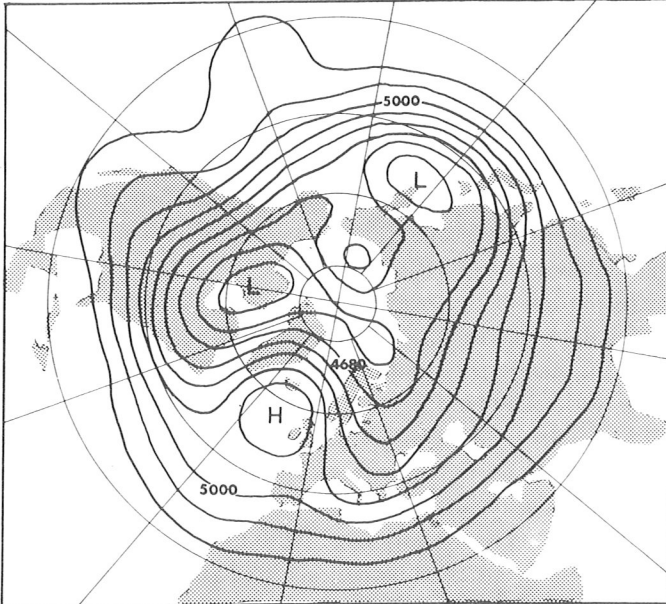
In Fig. 2 the distribution of the mean advection  $-\bar{V} \cdot \nabla \bar{\eta}$  is shown in the two cases. The oscillating nature of the mean vorticity field (not shown) along the mean jet axes ( $30^\circ - 40^\circ \text{N}$ ) is manifested in strong gradients in the advection term.

Fig. 3 shows the horizontal distribution of the vertically averaged vorticity forcing term  $\hat{k} \cdot \nabla \times A_H$ . Its order of magnitude ( $10^{-11} \text{ s}^{-2}$ ) is comparable to the advection term, but the two do not balance each other locally. Thus the mean vertical velocity is needed to maintain mean vorticity.

The  $\hat{k} \cdot \nabla \times A_H$  distribution shows very large latitudinal and longitudinal variability. This may arise (apart from numerical errors and the many derivations needed) from the good isotropy observed in the time-mean wind field: Use of spherical coordinates gives (HOLOPAINEN, [7]):

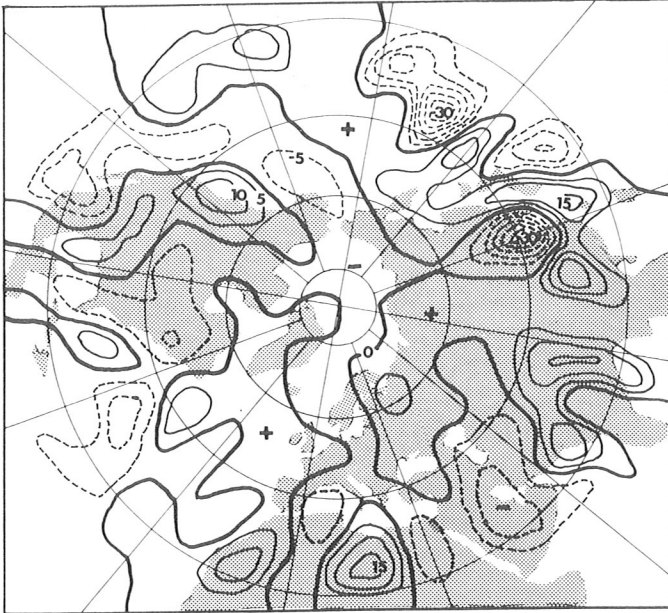


12/65

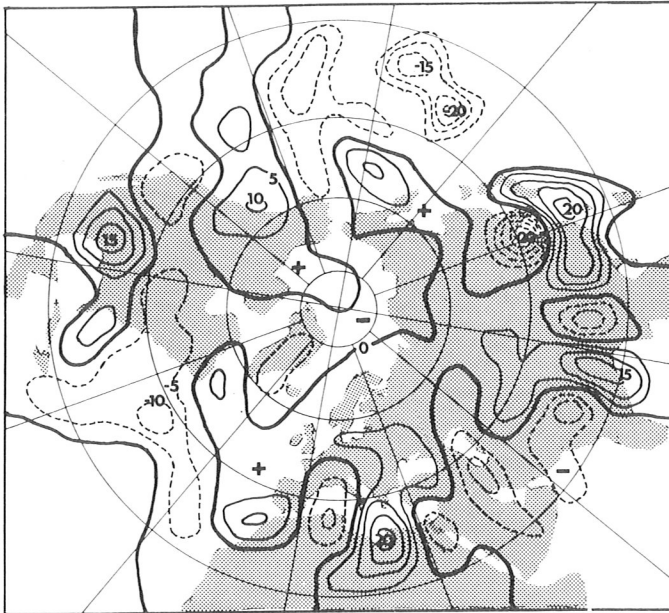


2/65

Fig. 1. Monthly mean height fields  $\bar{z}$  averaged vertically for the two periods in 1965. Unit: m.

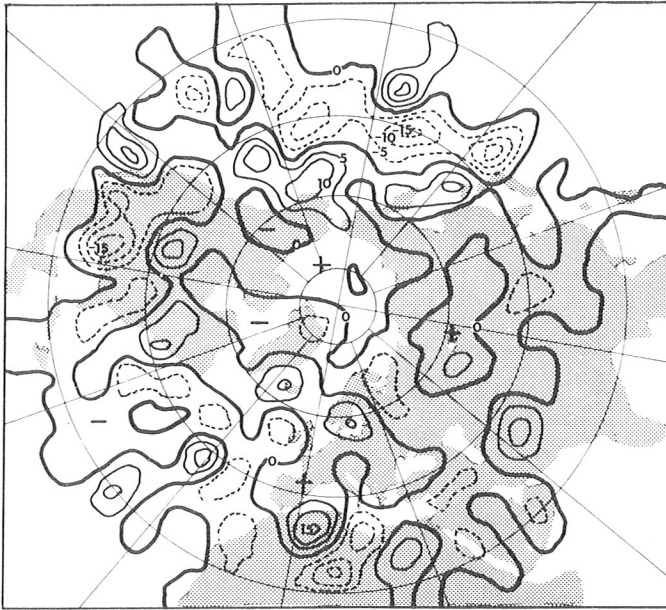


12/65

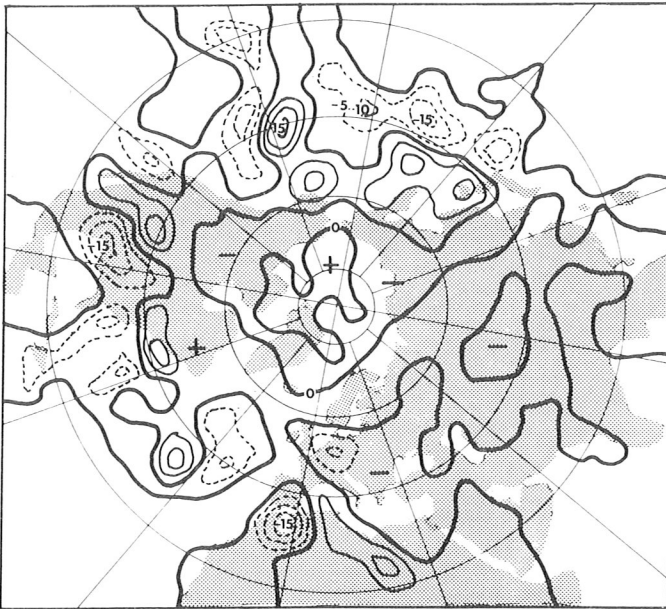


2/65

Fig. 2. Distribution of  $-\bar{V} \cdot \nabla \bar{\eta}$  averaged vertically. Unit:  $10^{-11} \text{ s}^{-2}$ .



12/65



2/65

Fig. 3. Distribution of  $\hat{k} \cdot \nabla \times A_H$  averaged vertically. Unit:  $10^{-11} \text{ s}^{-2}$ .

$$\begin{aligned} \hat{k} \cdot \nabla \times A_H = & \frac{1}{a^2 \cos^2 \varphi} \left( \frac{\partial}{\partial \varphi} \frac{1}{\cos \varphi} \frac{\partial}{\partial \varphi} \cos^2 \varphi - \frac{1}{\cos \varphi} \frac{\partial^2}{\partial \lambda^2} \right) \overline{u'v'} \\ & + \frac{1}{a^2 \cos^2 \varphi} \frac{\partial^2}{\partial \varphi \partial \lambda} \cos \varphi (\overline{u'^2} - \overline{v'^2}) \end{aligned} \quad (3.3)$$

$\hat{k} \cdot \nabla \times A_H$  is seen to be composed of only the anisotropic part of the horizontal wind statistics ( $\overline{u'v'}$ ,  $\overline{u'^2} - \overline{v'^2}$ ), which is smaller and probably more variable than the isotropic part.

The distribution has, however, some zonal symmetry. Large negative values are situated to the south in both cases, indicating an anticyclonizing effect in the areas of subtropical highs. Positive values (cyclonic forcing) are found in middle latitudes of cyclone activity. This indication of negative viscosity in a large-scale wind field is possibly related to the tendency of the cyclone tracks to deviate northwards and the anticyclone tracks southwards (PALMÉN & NEWTON, [10]).

There seems to be no great difference between the forcing terms in these two cases, not even in the blocking area. When these two monthly forcing distributions are compared with the calculations of HOLOPAINEN [7] for two 5-year periods and with those of PEIXOTO [12] for a six-month winter period it is seen that the main features are similar in all of them, *e.g.* the three anticyclonic forcing maxima along 30°N east of Japan, above the USA and along the West African coast. This type of kinematic forcing structure seems to be a regular feature of large scale turbulence, somewhat independent of the length of the period or type of circulation.

GREEN [6] has given an explanation of the maintenance of the strong anticyclone above England in July 1976. According to Green the eddies which go around the blocking pump anticyclonic vorticity to this area and thus help to maintain the blocking anticyclone. This feature, sometimes noticed by acting meteorologists, should be indicated by anticyclonic forcing by transients, *i.e.* negative values of  $\hat{k} \cdot \nabla \times A_H$ . In the 1965 blocking case there are no clearly negative values for this term in the anticyclone area; whether this is just a case where Green's mechanism was not crucial is not known. The calculations for 1976 data would give an interesting comparison.

The pressure-latitude distributions of  $[-\bar{V} \cdot \nabla \bar{\eta}]$  and  $[\hat{k} \cdot \nabla \times A_H]$  (brackets [ ] denoting zonal mean values) in the high index case are shown in Fig. 4. In the zonal mean values the vorticity forcing is the larger of the two in magnitude, especially in the upper troposphere, being positive between 45–70°N. This is in good agreement with the observed annual zonal angular momentum balance to which  $\hat{k} \cdot \nabla \times A_H$  is closely related through Eq. 3.3.

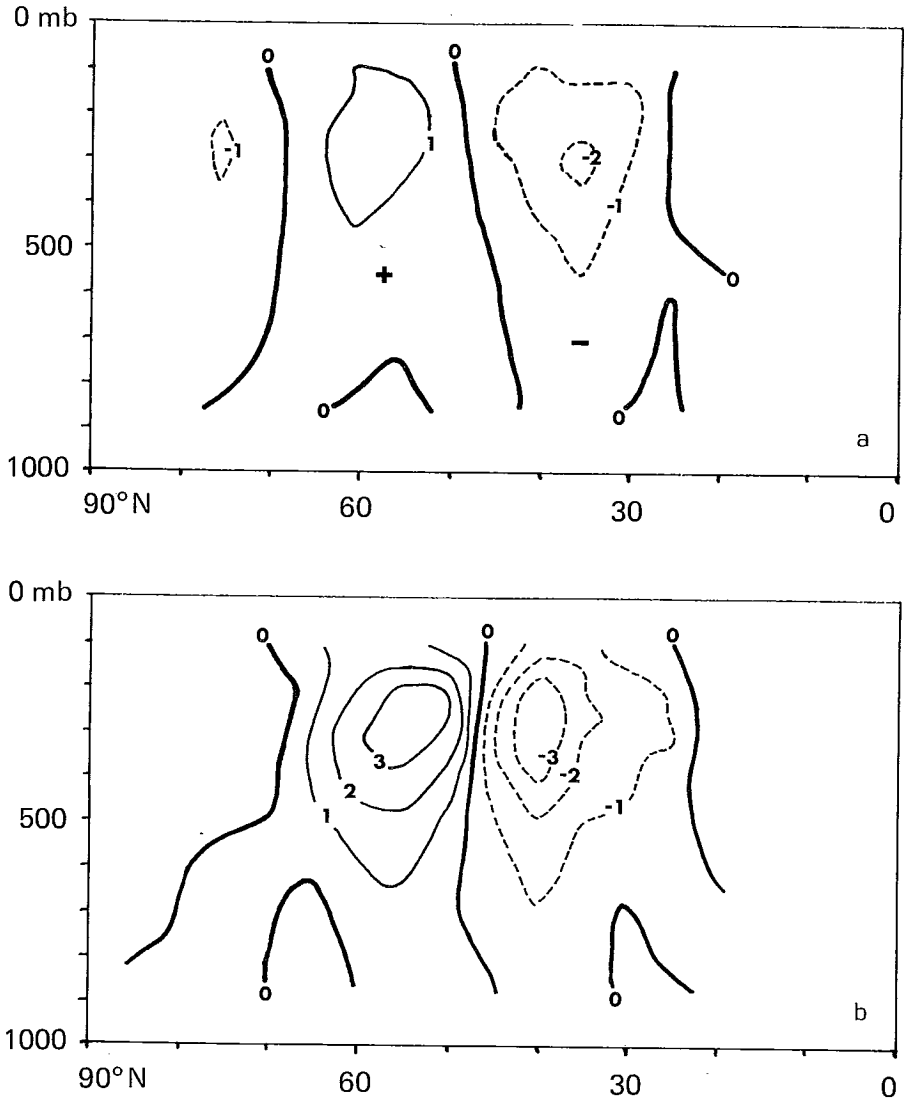


Fig. 4. Zonal averages for the high index case (12/1965). Unit:  $10^{-11} \text{ s}^{-2}$   
 a)  $[-\bar{V} \cdot \nabla \bar{\eta}]$       b)  $[\hat{k} \cdot \nabla \times A_H]$

The mean vertical velocity fields  $\bar{\omega}$ , obtained to balance Eq. 3.2., are shown in Fig. 5 for the two cases. At high and medium latitudes they look realistic, but south of  $40^\circ\text{N}$  there is strong variation due to the lack of »small« terms, which tend to be greater in tropics and due to large gradients in the  $-\bar{V} \cdot \nabla \bar{\eta}$ -field. The





12/65



2/65

Fig. 5. Distribution of  $\bar{\omega}$  averaged vertically. Unit:  $10^{-4} \text{ mb s}^{-1}$ . (Fourth order polynome fitting).

main features in the vertical average of  $\bar{\omega}$  are a downward motion ( $\bar{\omega} > 0$ ) in polar regions and an upward motion ( $\bar{\omega} < 0$ ) in the cyclone track areas along  $60^\circ\text{N}$  and around the blocking centre, magnitudes being  $\sim 1 \cdot 10^{-4} \text{ mb s}^{-1}$   $\sim 0.15 \text{ cm/s}$ . Fig. 6a shows the zonal mean values obtained by the polynome-

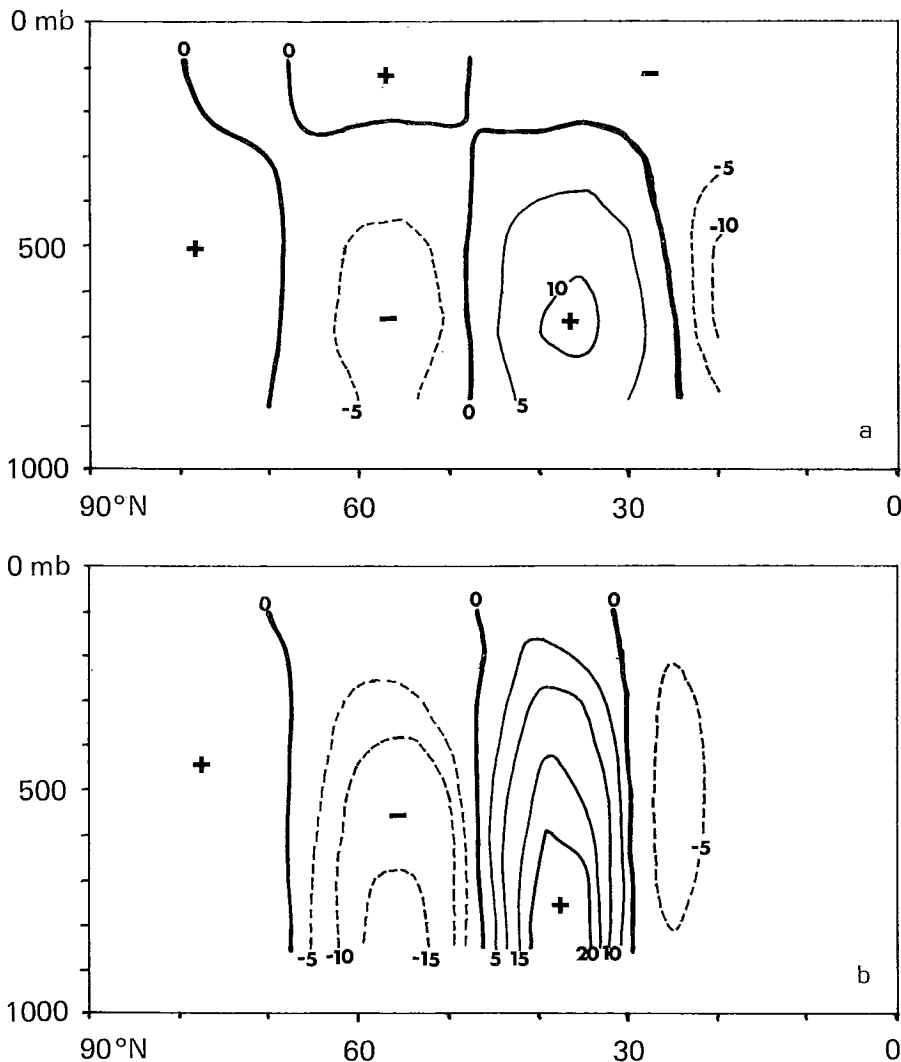


Fig. 6. Zonal averages of mean vertical velocity ( $\bar{\omega}$ ) for the high index case (12/1965). Unit:  $10^{-5} \text{ mb s}^{-1}$ .

a) Fourth order polynome fitting    b) Trapezoidal integration from above.

fitting method for  $[\bar{\omega}]$ . A corresponding value, using the trapezoidal rule for integration of  $\bar{\omega}$  from above ( $\bar{\omega} = 0$  at  $p = 0$ ), is given in Fig. 6b. They both show the three-cell structure, but the trapezoidal integration gives overly large values, especially in the lower troposphere, and does not change sign in the stratosphere.

#### 4. Temperature balance

In the time-mean temperature balance

$$\frac{\partial \bar{T}}{\partial t} = -\bar{V} \cdot \nabla \bar{T} - \nabla \cdot \overline{T'V'} + \overline{\sigma\omega} + \bar{Q} \quad (4.1)$$

where  $\sigma = -\frac{\partial T}{\partial p} + \frac{\alpha}{c_p}$  is the stability factor, the main interest has generally been in the transient term  $-\nabla \cdot \overline{T'V'}$  and in the mean diabatic heating  $\bar{Q}$ . There are many observational calculations of  $\bar{Q}$  based either on Eq. 4.1,  $\bar{Q}$  being computed as the residual needed to balance, or on approximations of the three main physical factors in the irreversible heating term: sensible heat exchange with the boundary, latent heat release and radiation effects. The residual method is used in this study, with the important independent  $\bar{\omega}$ -values taken from the previous chapter.

The monthly mean temperature field at the 500 mb level is shown in Fig. 7 together with the transient heat flux vectors  $\overline{T'V'}$ . The main function of the middle latitude weather disturbances is effectively to transport heat northwards. Being a fairly conservative property, (potential) temperature should show diffusive character even on long time scales. The flux vectors are indeed against the mean temperature gradient in middle latitudes, pointing towards lower mean temperature values, but they often also have a component parallel to the mean temperature isolines.

When the flux is formally divided into perpendicular and parallel components with regard to the mean isotherms,

$$\overline{T'V'} = -K \nabla \bar{T} + R \hat{k} \times \nabla \bar{T} \quad (4.2)$$

the coefficients  $K$  and  $R$  appear, where  $K$  is the along-gradient mixing coefficient and  $R$  the cross-gradient «rotational» coefficient according to CLAPP [4]. Figs. 8 and 9 show the two mixing coefficients for the two one-month periods, calculated from 500 mb data. The simplest parameterization theories assume  $K$  to be a positive constant. In the two cases  $K$  is mainly positive but variable. Its distribution has the same main features found by CLAPP [4] in vertically averaged 5-year data: large values above middle-latitude oceans and smaller, even negative values in the south.

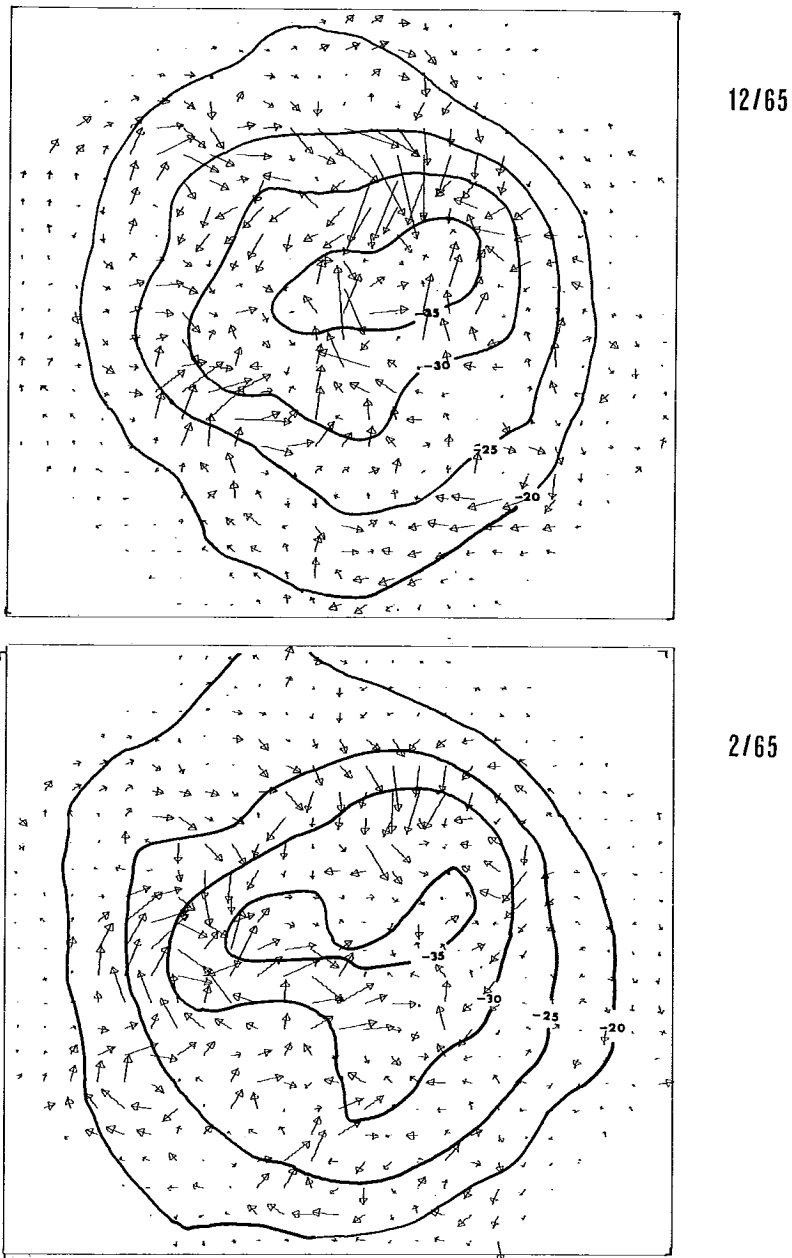
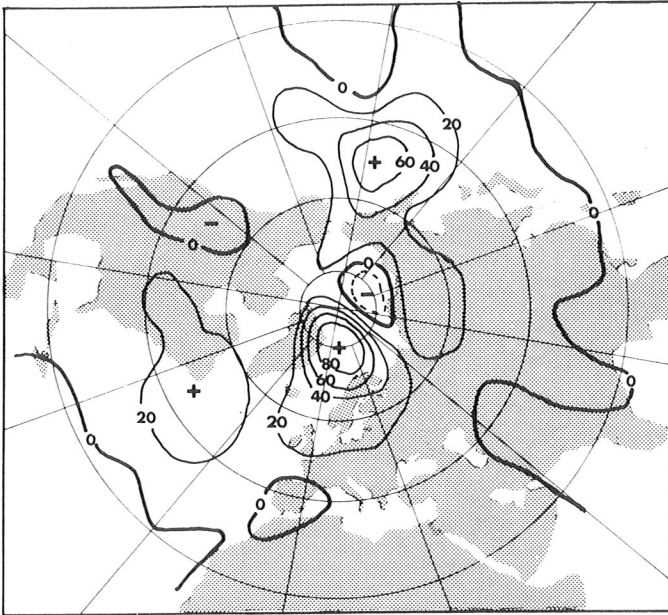
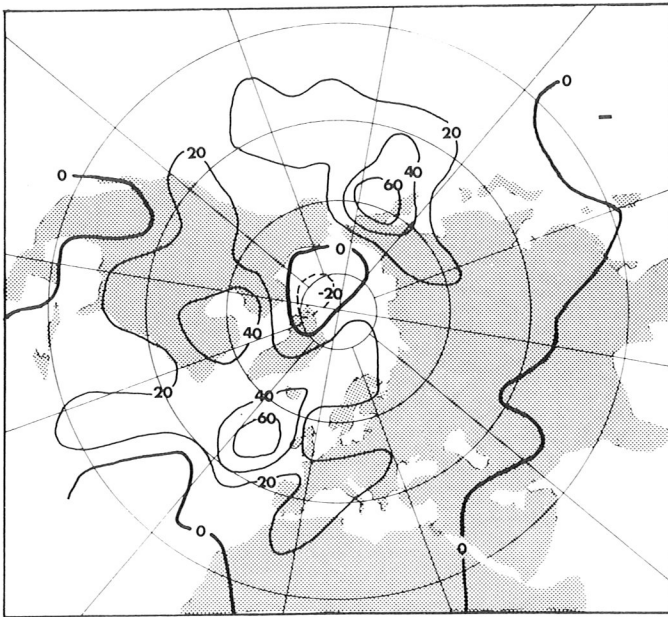


Fig. 7. Monthly mean 500 mb temperature  $\bar{T}$  (unit: °C) and transient heat flux vectors  $\overline{T'V'}$  (unit: grid length equals to 20 K ms<sup>-1</sup>).

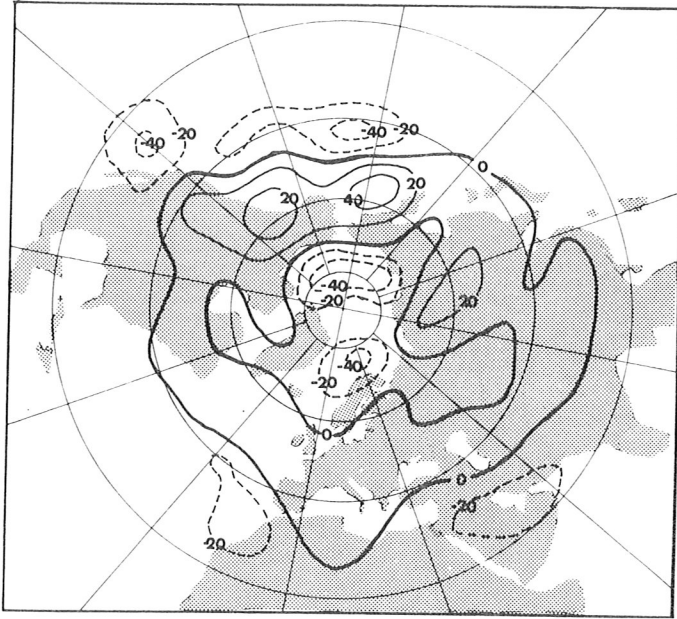


12/65

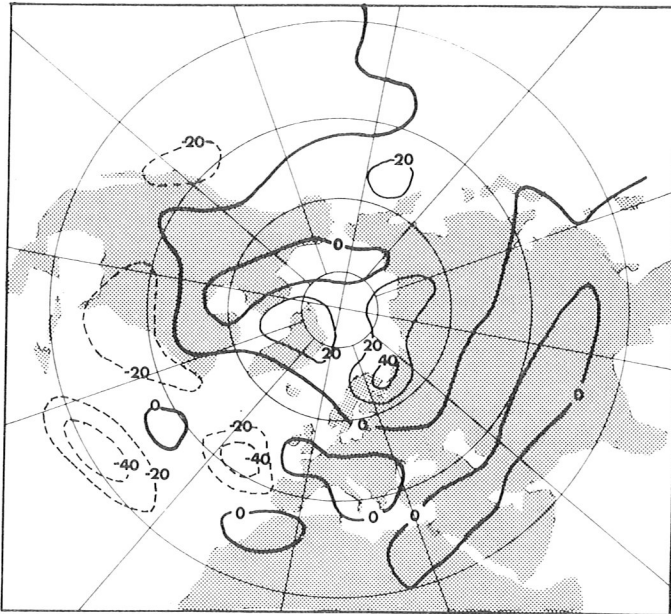


2/65

Fig. 8. Distribution of mixing coefficient  $K$ , 500 mb. Unit:  $10^5 \text{ m}^2 \text{ s}^{-1}$ .



12/65



2/65

Fig. 9. Distribution of rotational coefficient  $R$ , 500 mb. Unit:  $10^5 \text{ m}^2 \text{ s}^{-1}$ .

According to some elaborate theories (GREEN [5], STONE, [17]), based on baroclinical instability, the mixing coefficient for zonally averaged quantities should be proportional to the temperature gradient,  $K \propto \partial[\bar{T}]/\partial y$ . Although this roughly holds in zonally averaged data, the correlation between  $K$  and  $|\nabla\bar{T}|$  is small (0.07 over the grid) according to these cases. CLAPP [4] pointed out the role of topographic effects as a possible explanation for this discrepancy, but in the blocking case large  $K$  values are found in the warm Atlantic area where  $|\nabla\bar{T}|$  is small, and where topographic effects are absent. Moreover, large  $K$  values are systematically situated downstream from the maximum mean temperature gradients much like the kinetic energy of the transient motion.

Because the transient heat flux is the result of moving disturbances the intensity of the flow and especially that of its transient part could explain the mixing efficiency. The distributions of  $K$  and the kinetic energy of the transient mode of the flow,  $K_t = \frac{1}{2} \bar{V}'^2$  (Part I, Fig. 6) really have their maxima at roughly the same positions, especially in the blocking case (correlation  $r(K, K_t) = 0.32$ , areal mean of  $K = 1.13 \times 10^6 \text{ m}^2 \text{ s}^{-1}$ ), although the large maximum of  $K$  near Spitzbergen in the high index case has no corresponding  $K_t$  maximum ( $r(K, K_t) = 0.26$ , areal mean of  $K = 1.17 \times 10^6 \text{ m}^2 \text{ s}^{-1}$ ). This suggests the parameterization scheme  $\overline{T'V'} = -k \cdot \overline{V'^2} \cdot \nabla\bar{T}$  for the along-gradient component of the transient heat flux, thus interconnecting the motion and heat fields. There still remains the problem of parameterizing  $K_t$  and the parallel component using the mean variables  $\bar{T}$  and  $\bar{V}$ .

Considering the parallel component of the flux, CLAPP [4] discussed the macroscale extension of WELANDER'S [16] findings of microscale eddy transport of any quantity in rotating fluids. According to Welander there should be a parallel component to the mean isolines with  $R$  positive and proportional to the mean gradient. In the two cases here  $R$  is generally smaller in absolute values than  $K$ , somewhat polar symmetrical but mainly negative (areal means  $-3.92$  and  $-4.05 \times 10^5 \text{ m}^2 \text{ s}^{-1}$  for the high index and low index cases respectively), especially in the tropics. Its distribution shows large differences between the two cases and also with Clapp's results, indicating high variability in this flux property.

The vertical structure of zonally averaged  $K$  (Fig. 10a) shows that the negative («unmixing») values are concentrated in the middle latitude stratosphere. The maxima of  $R$  are situated near the tropopause (Fig. 10b) and positive values are concentrated at middle latitudes.

Although the transient heat flux is the basic property of the flow and its description even with the somewhat technical mixing concepts is essential, it is the flux divergence that contributes to the heat balance. This interaction term is given in Fig. 11. In both cases it is zonally symmetric, positive north from about

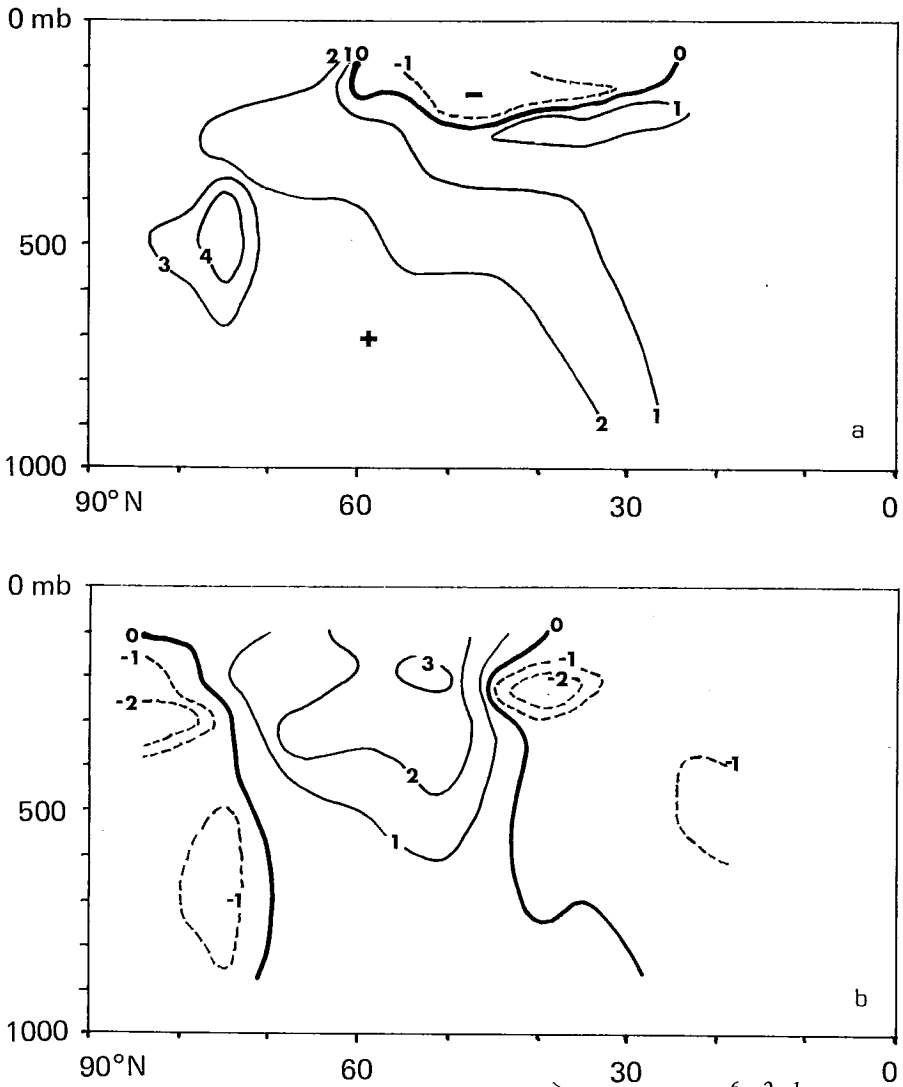


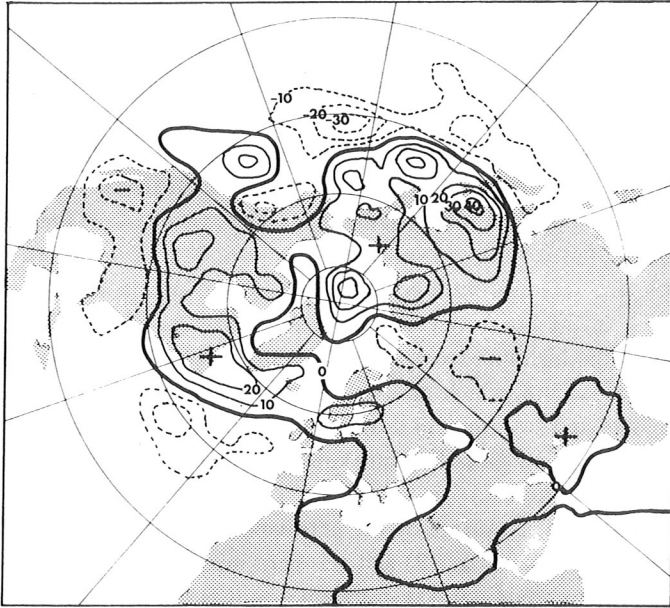
Fig. 10. Zonal averages for the high index case (12/1965). Unit:  $10^6 \text{ m}^2 \text{ s}^{-1}$ .

a) [ $K$ ]

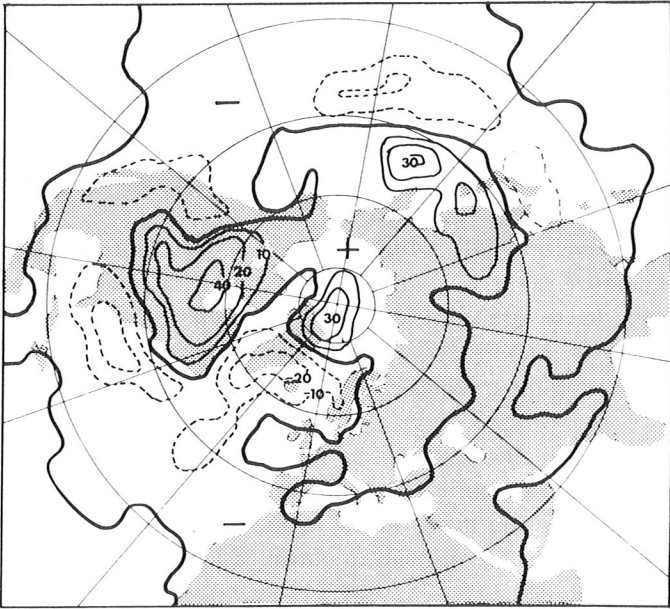
b) [ $R$ ]

$45^\circ\text{N}$ . The magnitudes are at the most  $4 \times 10^{-5} \text{ K s}^{-1}$  ( $\sim 4^\circ\text{C day}^{-1}$ ) which reflects the effectiveness of large-scale turbulence in the poleward heat transport at middle and high latitudes. The heating effect is at a maximum above eastern parts of the continents, in the areas of developing disturbances. In the blocking





12/65



2/65

Fig. 11. Distribution of  $-\nabla \cdot \overline{T'V'}$  averaged vertically. Unit:  $10^{-6} K s^{-1}$ .

case the most interesting feature is the strong negative area above the blocking anticyclone. As this area agrees well with the cyclone tracks for the period (PERRY [13], Fig. 4b) the moving disturbances have had a strong cooling effect even far in the north. The thermal forcing is thus more dependent on the type of circulation than the kinematic forcing  $\hat{k} \cdot \nabla \times A_H$ . The two are, however, somewhat similar in other respects, giving again an approximate connexion between kinematic and thermal properties of the transients — a fact that should be explained by theories for full-grown, large-scale disturbances. In the (nearer to normal) high-index case this term was similar to longer period calculations by e.g. PEIXOTO [11]. In the blocking case the vertical structure of the term was generally similar to the high-index case (Fig. 14a) in the troposphere but slightly different in the stratosphere, which may be a sign of stronger interaction between stratosphere and troposphere during an intense blocking episode. Sudden stratospheric warming, often preceding blocking (LABITZKE [8]), was not, however, found in January 1965.

Fig. 13 shows the vertical average of the net diabatic heating  $\bar{Q}$  needed to balance the sum of the mean (Fig. 12) and transient heat flux divergence and adiabatic mean heating  $\bar{\sigma}\bar{\omega}$ .  $\bar{\sigma}\bar{\omega}$ -term is not shown as it is  $\bar{\omega}$ -distribution weighted by upward and poleward increasing mean stability. The energetically important but probably smaller  $\bar{\sigma}'\bar{\omega}'$ -term was not available from the data.

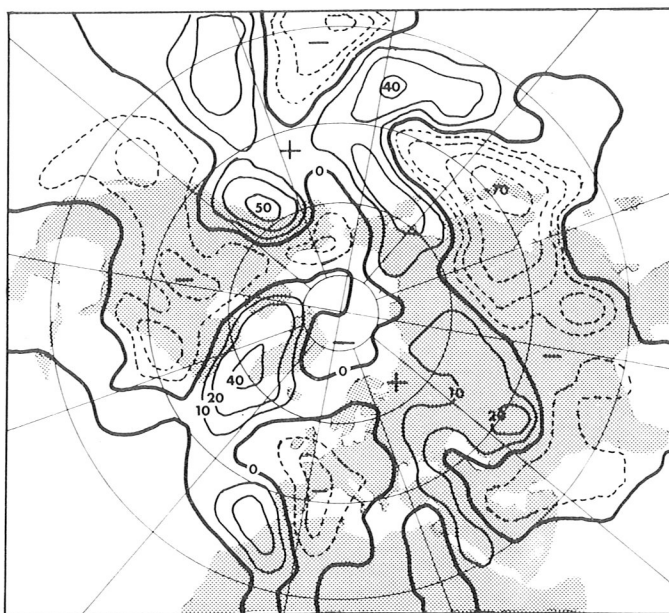
All the four terms in Eq. 4.1 are of the same magnitude and are important in the mean heat balance. The main feature in the  $\bar{Q}$ -distribution is the negative polar region due to polar night radiative cooling. Mean heat sources are found on the east coast of the U.S., South Asia and along the Pacific at 50°N extending in the north to Alaska. These features are also found in the studies by CLAPP [3], BROWN [2] and ASAKURA and KATAYAMA [1].

The vertical structure of  $\bar{Q}$  (Fig. 14b) is satisfactory at middle and high latitudes, where the large negative values are explained physically as infrared cooling. The small net heating at lower tropics could be explained as latent heat due to tropical rains but large upper tropical heating is contrary to the values obtained by NEWELL *et al.* [9], who calculated the combined effects of radiation and latent and sensible heating.

Part of the stratospheric heating could be explained as ozone absorption but, for the most part, the large positive values obtained indicate that the residual method is sensitive to errors in the balancing terms. The residual  $\bar{Q}$  is especially sensitive to the  $\bar{\omega}$ -field, which is difficult to obtain accurately.

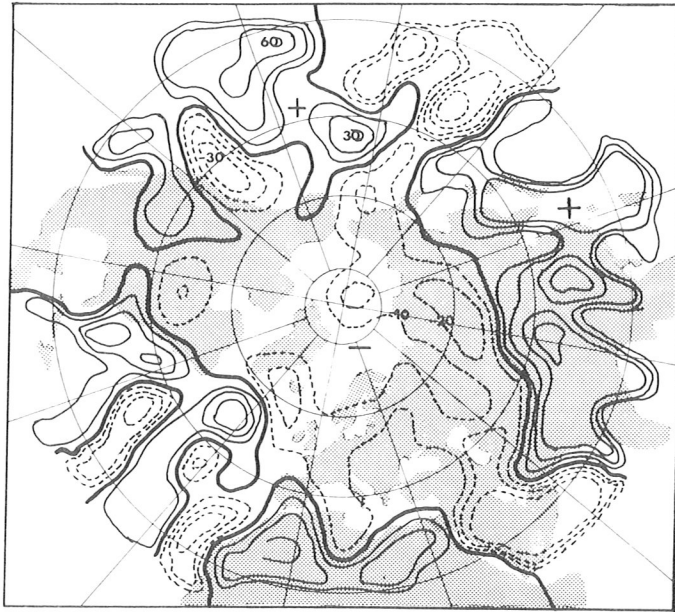


12/65



2/65

Fig. 12. Distribution of  $-\bar{V} \cdot \nabla \bar{T}$  averaged vertically. Unit:  $10^{-6} K s^{-1}$ .



12/65



2/65

Fig. 13. Distribution of  $\bar{Q}$  averaged vertically. Unit:  $10^{-6} K s^{-1}$ .

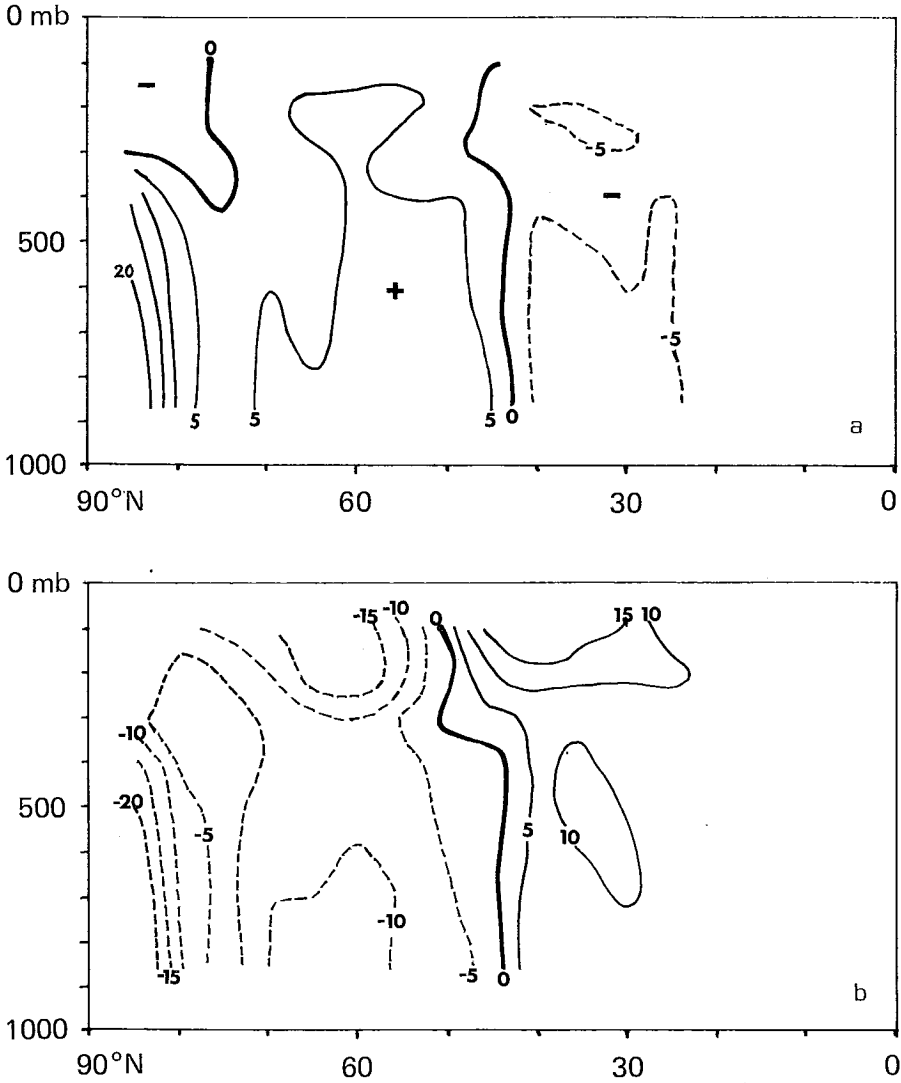


Fig. 14. Zonal averages for the high index case (12/1965). Unit:  $10^{-6} K s^{-1}$ .  
 a)  $[-\nabla \cdot \overline{T'V'}]$       b)  $\overline{Q}$

### 5. Conclusion

In the two one-month cases studied here, the effect of large-scale transient disturbances on the mean vorticity balance is locally very variable but important, especially at middle latitudes. The effect is somewhat similar to the corresponding term in the heat balance; both are mainly negative at low latitudes and positive at high latitudes. This vague similarity would suggest that a parameterization for the transient heat flux divergence *e.g.* by diffusive concepts would be a rough first approximation to the local kinematic forcing of the transients to mean vorticity field. This type of connection, between meridional momentum transport and the meridional temperature gradient,  $[\overline{u'v'}] = -K(z) \partial[\overline{T}]/\partial y$ , was used by WILLIAMS and DAVIES [19] in their mean motion model.

In the transient heat flux there exists a fairly large rotational component, and the along-gradient mixing coefficient is, according to the two cases, dependent on the flow field through the intensity of the eddies, measured by their kinetic energy. The effect of the disturbances is most intense around the baroclinic areas (above eastern continents) and is smaller elsewhere, even negative in the cyclone track area in front of the blocking anticyclone.

The time-mean temperature field is the most fundamental parameter to describe local climate. The large-scale turbulence affects this field in two ways: directly by the transient heat flux divergence and indirectly by contributing to the time-mean vertical velocity through vorticity balance conditions. Thus the climate is intimately related to the transients and even a small change — natural or man-made — in the cyclone routes may have a drastic effect on the local climate.

### REFERENCES

1. ASAKURA, T. and A. KATAYAMA, 1964: On the normal distribution of heat sources and sinks in the lower troposphere over the Northern Hemisphere. *J. Met. Soc. Japan*, **42**, 209–244.
2. BROWN, J.A., 1964: A diagnostic study of tropospheric diabatic heating and the generation of available potential energy. *Tellus*, **16**, 371–388.
3. CLAPP, P.F., 1961: Normal heat sources and sinks in the lower troposphere in winter. *Mon. Weath. Rev.*, **89**, 147–162.
4. —, 1970: Parameterization of macroscale transient heat transport for use in a mean motion model of the general circulation. *J. Appl. Met.*, **9**, 554–563.
5. GREEN, J.S.A., 1970: Transfer properties of the large-scale eddies and the general circulation of the atmosphere. *Q. J.R.M.S.*, **96**, 157–185.
6. —, 1977: The weather during July 1976: Some dynamical considerations of the draught. *Weather*, **32**, 120–126.

7. HOLOPAINEN, E.O., 1975: Diagnostic studies on the interaction between the time-mean flow and the large-scale transient fluctuations in the atmosphere. *Dept. of Meteorology, Univ. of Helsinki, Report No. 8*, 14 pp.
8. LABITZKE, K.B., 1965: On the mutual relation between stratospheric warming in winter. *J. Appl. Met.*, 4, 91–99.
9. NEWELL, R., KIDSON, J., VINCENT, D. and G. BOER, 1972: *The general circulation of the tropical atmosphere*. M.I.T. Press, London.
10. PALMÉN, E. and C.W.P. NEWTON, 1969: *Atmospheric Circulation Systems*. Academic Press, London.
11. PEIXOTO, J.P., 1960: Hemispheric temperature conditions during the year 1950. *Sci. Rept. No. 4, Planetary Circulation Project, M.I.T.*
12. —, 1971: The forcing function for large scale mean perturbances of the general circulation of the atmosphere. *Publication No. 9, Univ. of Lisboa, Instituto Geofísico do Infante D. Luis*.
13. PERRY, A.H., 1968: Turbulent heat flux patterns over the North Atlantic during recent winter months. *Met. Mag.*, 97, 246–254.
14. PERRY, J.S., 1967: Long wave energy processes in the 1963 sudden stratospheric warming. *J. Atm. Sc.*, 24, 539–550.
15. SALTZMAN, B., 1962: Empirical forcing functions for the large-scale mean disturbances in the atmosphere. *Geof. Pura e Appl.*, 52, 173–188.
16. SAVIJÄRVI, H., 1976: The interaction of the monthly mean flow and large-scale transient eddies in two different circulation types, Part I. *Geophysica*, 14, 23–46.
17. STONE, P., 1973: The effect of large-scale eddies on climatic change. *J. Atm. Sc.*, 30, 521–529.
18. WELANDER, P., 1966: Note on the effect of rotation on diffusion processes. *Tellus*, 18, 63–66.
19. WILLIAMS, G.P. and D.R. DAVIES, 1965: A mean motion model of the general circulation. *Q. J.R.M.S.*, 91, 471–489.